

ADAPTIVE FINITE STATE PROJECTION WITH QUANTILE-BASED PRUNING FOR SOLVING THE CHEMICAL MASTER EQUATION

ADITYA DENDUKURI AND LINDA PETZOLD*

Abstract. We present an adaptive Finite State Projection (FSP) method for efficiently solving the Chemical Master Equation (CME) with rigorous error control. Our approach integrates time-stepping with dynamic state-space truncation, balancing accuracy and computational cost. Krylov subspace methods approximate the matrix exponential, while quantile-based pruning controls state-space growth by removing low-probability states. Theoretical error bounds ensure that the truncation error remains bounded by the pruned mass at each step, which is user-controlled, and does not propagate forward in time. Numerical experiments on biochemical systems, including the Lotka–Volterra and Michaelis–Menten and bi-stable toggle switch models.

Key words. chemical master equation, finite state projection, discrete stochastic simulation, stochastic simulation algorithm

AMS subject classifications. 60H35, 65C40, 65F10

1. Introduction. Understanding the stochastic dynamics of biochemical reaction networks is crucial in systems biology, synthetic biology, and chemical engineering. These dynamics are rigorously described by the Chemical Master Equation (CME), which represents the time evolution of a probability distribution over a discrete state space. Each state corresponds to a specific combination of molecule counts for the involved chemical species, and transitions occur randomly according to reaction propensities, resulting in a continuous-time Markov process. However, solving the CME directly is often computationally intractable due to the curse of dimensionality—the exponential growth of possible system states with the number of chemical species. Traditionally, trajectory-based methods such as Gillespie’s stochastic simulation algorithm (SSA) [8, 9] have been widely employed to approximate solutions to the CME. These methods simulate individual trajectories to estimate the evolving probability distribution but become computationally prohibitive for high-dimensional systems or when rare events must be accurately characterized.

An important observation for practical biochemical systems is the natural sparsity of their probability distributions—most of the theoretically infinite state space carries zero or negligible probability. Exploiting this sparsity, the Finite State Projection (FSP) method [14] projects the infinite-dimensional state space onto a finite, computationally manageable subset, rigorously bounding the truncation error. Specifically, if the retained subset captures at least $(1 - \varepsilon)$ of the total probability, the computed solution is guaranteed to be within an error ε of the true CME solution.

Since the original development of the FSP method, significant advancements have focused on adaptive truncation techniques. Methods such as the sliding window approach [21] dynamically adjust the state space by tracking probability flow, while SSA-driven expansion techniques [5, 17, 13] use short simulations to predict relevant states. Traditional pruning approaches typically employ fixed thresholds to remove states with probabilities below a certain cutoff. However, such methods can lead to excessive pruning in sparse regions or insufficient pruning in dense regions as the distribution evolves over time.

*Department of Computer Science, University of California, Santa Barbara (aditya_dendukuri@ucsb.edu, petzold@ucsb.edu).

Beyond traditional truncation methods, alternative strategies have emerged. Slack reactant methods introduce effective state-space boundaries by modifying reaction networks [12]. Partitioning species into molecular equivalence groups (MEGs) with reflecting boundaries provides *a priori* error estimates [3]. Adaptive basis selection methods employing wavelet or orthogonal polynomial representations compress probability distributions into dynamically refined bases [10], and tensor decomposition methods, such as Quantized Tensor Trains (QTT), address dimensionality issues by compressing high-dimensional CME solutions [11, 20, 6].

Complementing these truncation strategies, Krylov subspace methods significantly enhance the efficiency of solving the CME by approximating the action of matrix exponentials, essential to FSP computations [16]. Early work by Burrage *et al.* [2] demonstrated the feasibility of integrating Krylov-based solvers with FSP, while subsequent improvements in adaptive subspace dimensioning and incomplete orthogonalization have yielded faster and more stable solvers [19]. These developments facilitate larger time steps and improved handling of stiffness, crucial for analyzing complex biochemical reaction networks.

In this paper, we build upon previous CME solution methods by developing a FSP framework with quantile-based pruning. Our approach combines elements of optimal FSP (which minimizes state space size) and time-stepping FSP methods, while incorporating a simple yet effective modification: instead of using fixed probability thresholds for state pruning, we remove a fixed *fraction* of the least probable states (e.g., the bottom 5%) at each time step, followed by renormalization. This quantile-based strategy adapts to the current shape of the probability distribution—preventing over-pruning in sparse distributions and under-pruning in dense ones—providing improved stability across diverse systems and time scales. By integrating this quantile-based pruning with Krylov subspace integration and balancing pruning and time-stepping errors, our framework offers a practical balance between computational efficiency and accuracy. We analyze the mathematical properties of this approach, showing that well-controlled global error bounds can be maintained despite the pruning and renormalization operations.

The remainder of this paper is organized as follows. In Section 2, we introduce the CME and FSP methods, establishing our mathematical foundation. Section 3 details our approach, integrating quantile-based pruning with controlled error bounds for dynamic state-space adjustment. Section 3.3 rigorously analyzes truncation and integration errors, establishing theoretical guarantees on global accuracy. In Section 3.6, we present our FSP algorithm with quantile-based pruning, incorporating these error bounds to guide state-space updates. Finally, Section 5 validates our method through numerical experiments on benchmark stochastic biochemical models, demonstrating its robustness and computational advantages.

2. Background and Notation.

DEFINITION 2.1 (Chemical Reaction Network). A **Chemical Reaction Network** consists of N species and M reactions. Each reaction can be expressed as:

$$\begin{aligned} a_{11}x_1 + \cdots + a_{1N}x_N &\longrightarrow b_{11}x_1 + \cdots + b_{1N}x_N, \\ &\vdots \\ a_{M1}x_1 + \cdots + a_{MN}x_N &\longrightarrow b_{M1}x_1 + \cdots + b_{MN}x_N, \end{aligned} \tag{2.1}$$

where a_{ij} and b_{ij} are stoichiometric coefficients, and x_i represents the population count of species i .

The reaction network can also be expressed in matrix form as:

$$(2.2) \quad \underbrace{\begin{pmatrix} a_{11} & \cdots & a_{1M} \\ \vdots & \ddots & \vdots \\ a_{N1} & \cdots & a_{NM} \end{pmatrix}}_{\mathbf{A}} \underbrace{\begin{pmatrix} x_1 \\ \vdots \\ x_N \end{pmatrix}}_{\mathbf{x}} \rightarrow \underbrace{\begin{pmatrix} b_{11} & \cdots & b_{1N} \\ \vdots & \ddots & \vdots \\ b_{M1} & \cdots & b_{MN} \end{pmatrix}}_{\mathbf{B}} \underbrace{\begin{pmatrix} x_1 \\ \vdots \\ x_N \end{pmatrix}}_{\mathbf{x}}.$$

DEFINITION 2.2 (Stoichiometric Matrix). The **Stoichiometric Matrix**, \mathbf{S} , is defined as:

$$(2.3) \quad \mathbf{S} := \mathbf{B} - \mathbf{A},$$

where each column vector $\boldsymbol{\nu}_i$ corresponds to the net change in species populations for reaction i . Thus:

$$(2.4) \quad \mathbf{S} = \left(\begin{array}{c|c|c|c|c} | & | & | & \cdots & | \\ \boldsymbol{\nu}_1 & \boldsymbol{\nu}_2 & \boldsymbol{\nu}_3 & \cdots & \boldsymbol{\nu}_M \\ | & | & | & & | \end{array} \right).$$

DEFINITION 2.3 (System State). The **System State** is represented by a vector \mathbf{x} that contains the copy numbers of each species:

$$(2.5) \quad \mathbf{x} := \begin{pmatrix} x_1 \\ x_2 \\ \vdots \\ x_N \end{pmatrix},$$

where x_i denotes the population of species i .

DEFINITION 2.4 (State Space). The **State Space**, \mathbf{X} , is the set of all possible states the system can occupy.

For example, given a system with two species, the state space is:

$$(2.6) \quad \mathbf{X} := \left\{ \begin{pmatrix} 0 \\ 0 \end{pmatrix}, \begin{pmatrix} 0 \\ 1 \end{pmatrix}, \begin{pmatrix} 0 \\ 2 \end{pmatrix}, \cdots, \begin{pmatrix} \infty \\ \infty \end{pmatrix} \right\}.$$

DEFINITION 2.5 (Probability Distribution over State Space). Given a state $\mathbf{x} \in \mathbf{X}$, $\mathbf{p}(\mathbf{x}, t)$ represents the probability of system being at state \mathbf{x} at time t .

DEFINITION 2.6 (Chemical Master Equation (CME)). The **Chemical Master Equation (CME)** describes the time evolution of the probability distribution $\mathbf{p}(\mathbf{x}, t)$ over the state \mathbf{x} . For a single state \mathbf{x} , the CME is:

$$(2.7) \quad \frac{d}{dt} \mathbf{p}(\mathbf{x}, t) = \sum_{k=1}^M \alpha_k(\mathbf{x} - \boldsymbol{\nu}_k) \mathbf{p}(\mathbf{x} - \boldsymbol{\nu}_k) - \alpha_k(\mathbf{x}) \mathbf{p}(\mathbf{x}),$$

where $\alpha_k(\mathbf{x})$ represents the propensity function for reaction k at state \mathbf{x} .

For the entire state space \mathbf{X} , the CME is expressed as:

$$(2.8) \quad \frac{d}{dt} \mathbf{p}(\mathbf{X}, t) = \mathbf{A} \mathbf{p}(\mathbf{X}, t),$$

where $\mathbf{p}(\mathbf{X}, t)$ is the probability distribution over \mathbf{X} at time t , and the matrix \mathbf{A} is defined as:

$$(2.9) \quad \mathbf{A}_{ij} = \begin{cases} \sum_{k=1}^M \alpha_k(\mathbf{X}_i), & \text{if } i = j, \\ \alpha_k(\mathbf{X}_j), & \text{if } \mathbf{X}_i = \mathbf{X}_j + \boldsymbol{\nu}_k, \\ 0, & \text{otherwise.} \end{cases}$$

DEFINITION 2.7 (Finite State Projection). The **Finite State Projection (FSP)** method approximates the solution of the CME by reducing the infinite state space \mathbf{X} to a finite subset $\mathbf{X}_J \subset \mathbf{X}$. The solution is computed as:

$$(2.10) \quad \mathbf{p}(\mathbf{X}_J, t) \approx e^{\mathbf{A}_J t} \mathbf{p}(\mathbf{X}, 0),$$

where \mathbf{A}_J is the truncated transition matrix.

2.1. FSP Algorithm. The algorithm, detailed in 2.1, begins by initializing the finite state space \mathbf{X}_J with the initial state \mathbf{x}_0 and assigning it a probability of one. It then enters an iterative loop where, at each step, new states are added to \mathbf{X}_J to capture additional probability mass. Following the expansion of the state space, the corresponding transition matrix \mathbf{A}_J is assembled to represent the possible transitions between states. The probability distribution $\mathbf{p}(\mathbf{X}_J, t)$ is subsequently approximated by computing the matrix exponential $e^{\mathbf{A}_J t} \mathbf{p}(\mathbf{X}_J, 0)$. This iterative process continues until the cumulative probability mass outside the finite state space falls below the predefined error tolerance ϵ . By systematically expanding the state space and updating the transition matrix, the standard FSP algorithm ensures an accurate and computationally efficient approximation of the system's stochastic dynamics.

Algorithm 2.1 Standard FSP Algorithm [14]

Inputs: Time interval (t_0, t_f) , initial state \mathbf{x}_0 , error tolerance ϵ .
Initialize $\mathbf{X}_J = \{\mathbf{x}_0\}$, $\mathbf{p}(\mathbf{X}_J, 0) = [1]$.
while $\mathbf{1}^T \mathbf{p}(\mathbf{X}_J, t) > \epsilon$ **do**
 Add new states to \mathbf{X}_J .
 Assemble the transition matrix \mathbf{A}_J .
 Compute $\mathbf{p}(\mathbf{X}_J, t) \approx e^{\mathbf{A}_J t} \mathbf{p}(\mathbf{X}_J, 0)$.
end while
return $\mathbf{p}(\mathbf{X}_J, t)$.

2.2. FSP with Time Stepping. The Time-Stepping FSP is a variant of the FSP algorithm that solves the CME incrementally over discrete time intervals rather than solving directly for the entire time domain 2.2. This approach allows the state space \mathbf{X}_J to adapt dynamically at each time step based on the system's behavior, ensuring that only the relevant states are included in the computation. At each step, the probability distribution is advanced using matrix exponentiation within the finite subspace, and the truncation error is checked. If necessary, the state space is expanded to capture sufficient probability mass, providing a balance between accuracy and computational efficiency. This time-stepping approach is particularly advantageous for systems with transient dynamics or varying levels of activity over time.

Algorithm 2.2 FSP with Time Stepping [15]

INPUTS: time interval (t_0, t_f) , initial state \mathbf{x}_0 , error tolerance ϵ , step size δt
 Define $t := t_0$, $\mathbf{X}_J = \{\mathbf{x}_0\}$, $\mathbf{p}(\mathbf{X}_J, 0) = [1]$
while $t < t_f$ **do**
 Use the standard FSP algorithm 2.1 for time interval $(t, t + \delta t)$
 $t = t + \delta t$
end while
return $\mathbf{p}(\mathbf{X}_J, t)$

2.3. Optimal FSP. The traditional finite state projection (FSP) approach becomes computationally intractable over long time scales due to the exponential growth of the state space \mathbf{X}_J . As the system evolves, older states quickly become negligible, while new states continuously emerge, further expanding the state space and making the direct application of FSP increasingly inefficient. Therefore, it is crucial to develop strategies that control the size of the state space, ensuring that only the most significant states are retained for accurate and efficient simulation of the system. The optimal FSP algorithm enhances the traditional Finite State Projection approach for solving the Chemical Master Equation by employing an adaptive and optimization-driven framework for state space truncation. Unlike conventional FSP methods that use fixed criteria to limit the state space, Optimal FSP dynamically selects and prioritizes states based on their probabilistic significance through an iterative optimization process.

$$J' = \arg \min_{J' \subset J_{k+1}} \left| \mathbf{1}^T \mathbf{p}(\mathbf{X}_{J'}, t_{k+1}) - \frac{\epsilon_k}{2} \right|,$$

Algorithm 2.3 details the optimal FSP method:

This method formulates state selection as an optimization problem, aiming to maximize captured probability mass while minimizing computational resources, often utilizing linear or convex optimization techniques. Additionally, Optimal FSP integrates rigorous error control mechanisms to ensure that the truncation error remains within predefined tolerances, thereby maintaining the accuracy of the probability distribution approximation. Hierarchical partitioning of the state space further enables the method to efficiently handle high-dimensional and complex biochemical networks by decomposing them into manageable subsets. Efficient matrix construction and updates are achieved through advanced sparse matrix algorithms, ensuring scalability and computational feasibility. Overall, Optimal FSP provides a more accurate and computationally efficient solution to stochastic chemical kinetics problems, making it a valuable tool for researchers in systems biology and related fields.

3. Adaptive FSP with Quantile-Based Pruning. In this section, we introduce our adaptive method for solving the Chemical Master Equation (CME) efficiently. A fixed probability cutoff—removing all states with probability below a certain threshold—can be unreliable when the overall probability distribution changes drastically over time. By contrast, a *quantile-based* (or percentile-based) pruning strategy dynamically removes a fixed *fraction* α of the least probable states (for instance, the bottom 5%) at each time step. This approach prevents over-pruning in sparse distributions and under-pruning in dense ones by adapting to the current shape of the distribution. Our approach combines quantile-based pruning with an adaptive time-stepping strategy, ensuring that the truncation error remains bounded and con-

Algorithm 2.3 Optimal FSP Method [17]

- 1: **Inputs:** \mathbf{X}_{J_k} (state space at t_k), τ_k (time step), ϵ_k (tolerance).
- 2: **Step 0: Initialization.**
- 3: Start with \mathbf{X}_{J_k} , τ_k , ϵ_k .
- 4: **Step 1: State expansion.**

$$J_{k+1} = \text{Expand}(\mathbf{X}_{J_k}, r) \quad \text{such that} \quad 1 - \mathbf{1}^T \mathbf{p}_{k+1}(t_{k+1}) < \frac{\epsilon_k}{2}.$$

- 5: **Step 2: State pruning.**

$$J' = \arg \min_{J' \subset J_{k+1}} \left| \mathbf{1}^T \mathbf{p}(\mathbf{X}_{J'}, t_{k+1}) - \frac{\epsilon_k}{2} \right|,$$

where J' is constructed by removing states with the smallest probabilities in $\mathbf{p}_{k+1}(t_{k+1})$.

- 6: **Step 3: State truncation.**

$$J_{k+1} = J_{k+1} \setminus J',$$

such that:

$$1 - \mathbf{1}^T \mathbf{p}_{k+1}(t_{k+1}) < \epsilon_k.$$

trolled by the user. We derive rigorous error bounds that link the pruned probability mass to the global solution error, allowing us to develop an algorithm that dynamically adjusts the state space while maintaining accuracy. Theoretical analysis follows, demonstrating that error propagation remains well-behaved under this framework. Finally, we discuss implementation details, including efficient quantile selection, matrix updates, and renormalization.

3.1. Quantile Selection Process. Let $\mathbf{p}(\mathbf{X}_S, t)$ denote the probability distribution over a finite subset $\mathbf{X}_S \subset \mathbf{X}$, where \mathbf{X}_S is our current truncated state space. For $x \in \mathbf{X}_S$, let $p(x, t)$ denote the probability of state x at time t . By definition,

$$\sum_{x \in \mathbf{X}_S} p(x, t) = 1.$$

The quantile-based pruning method seeks to identify and remove a subset $\mathbf{X}_{\text{prune}} \subset \mathbf{X}_S$ whose total probability mass is at most $\alpha \in (0, 1)$. Equivalently, $\mathbf{X}_{\text{prune}}$ represents the bottom α -fraction of states by probability. This ensures that the removal affects no more than a fraction α of the distribution, thereby providing a direct bound on the truncation error.

To determine which states to remove, we (1) order the states by probability, (2) compute the cumulative distribution, and (3) identify the smallest index covering probability α . Concretely, for a given time t , arrange the states as

$$p(x_1, t) \leq p(x_2, t) \leq \dots \leq p(x_N, t),$$

where $N = |\mathbf{X}_S|$. Define the cumulative mass:

$$P_{\text{cumulative}}(k, t) = \sum_{i=1}^k p(x_i, t), \quad k = 1, \dots, N.$$

Then choose the index k^* such that

$$P_{\text{cumulative}}(k^*, t) \geq \alpha \quad \text{and} \quad P_{\text{cumulative}}(k^* - 1, t) < \alpha.$$

In practice, we set $q_\alpha = p(x_{k^*}, t)$. All states with probabilities $\leq q_\alpha$ are then included in

$$\mathbf{X}_{\text{prune}} = \{x_1, \dots, x_{k^*}\}.$$

Remark 3.1 (Handling Ties). If several states around the cutoff α share the same probability, all of them will be pruned. Consequently, the total pruned mass m can satisfy $m \geq \alpha$. In practice, m is usually very close to α , but this effect should be noted when tight control over the total truncated mass is crucial.

3.2. Algorithmic Implementation. Algorithm 3.1 summarizes the practical steps for identifying and removing states whose probability is at or below q_α . A naive implementation requires a full sort of state probabilities, which costs $O(N \log N)$. For large-scale systems, one can accelerate the quantile determination by using a partial sort or quickselect-based routine, yielding an $O(N)$ average complexity.

Algorithm 3.1 Quantile-Based Pruning (Bottom- α Fraction)

Require: Current truncated state space \mathbf{X}_S , probability vector $\{p(x, t)\}_{x \in \mathbf{X}_S}$, target fraction α

- 1: Determine the number of states $N = |\mathbf{X}_S|$
- 2: Use a selection or sorting routine to find q_α such that the total probability of all states with $p(x, t) \leq q_\alpha$ is at most α
- 3: Define

$$\mathcal{R} = \{x \in \mathbf{X}_S : p(x, t) \leq q_\alpha\}$$

- 4: Remove the states in \mathcal{R} (i.e., set their probabilities to 0)
- 5: Let $m = \sum_{x \in \mathcal{R}} p(x, t)$
- 6: Renormalize the remaining probabilities to sum to 1:

$$p'(x, t) \leftarrow \frac{p(x, t)}{1 - m} \quad \text{for all } x \in \mathbf{X}_S \setminus \mathcal{R}$$

- 7: **return** Updated probability vector $\{p'(x, t)\}$ and updated truncated state space $\mathbf{X}_S \setminus \mathcal{R}$
-

Although Algorithm 3.1 can be applied at every time step, frequent sorting or partial-sorting can become computationally expensive. A practical strategy is to prune only when needed—e.g., after a fixed number of time steps or when the proportion of negligible states exceeds a predetermined threshold.

Remark 3.2 (Renormalization). After removing low-probability states, one must rescale the probabilities of the remaining states so that they sum to one. Specifically, if \mathcal{R} is the pruned set with total mass m , define

$$p'(x, t) = \begin{cases} p(x, t), & x \notin \mathcal{R}, \\ 0, & x \in \mathcal{R}, \end{cases}$$

and set

$$\mathbf{p}(\mathbf{X}_S \setminus \mathcal{R}, t) = \frac{\mathbf{p}'(t)}{1 - m}.$$

Renormalization ensures that the updated probability distribution still satisfies the Kolmogorov axioms. This procedure does not invalidate the ℓ^1 -error bounds described below (see Proposition 3.4).

3.3. Truncation Error Analysis. We now analyze how removing a fraction α of states (by probability mass) affects the solution accuracy. Let the full state space be \mathbf{X} and partition it as

$$\mathbf{X} = S \cup R, \quad S \cap R = \emptyset,$$

where $S \subset \mathbf{X}$ is the truncated (finite) set of states we keep, and $R = \mathbf{X} \setminus S$ is the remainder. Denote by $\mathbf{p}_S(t)$ and $\mathbf{p}_R(t)$ the probability vectors restricted to S and R , respectively.

Remark 3.3. For a Chemical Master Equation (CME) with generator matrix \mathbf{A} , one can partition the equation as

$$\frac{d}{dt} \begin{pmatrix} \mathbf{p}_S(t) \\ \mathbf{p}_R(t) \end{pmatrix} = \begin{pmatrix} \mathbf{A}_{SS} & \mathbf{A}_{SR} \\ \mathbf{A}_{RS} & \mathbf{A}_{RR} \end{pmatrix} \begin{pmatrix} \mathbf{p}_S(t) \\ \mathbf{p}_R(t) \end{pmatrix},$$

where \mathbf{A}_{SS} and \mathbf{A}_{RR} represent transitions within S and R , respectively, while \mathbf{A}_{SR} and \mathbf{A}_{RS} represent transitions between these sets, as illustrated in Figure 1.

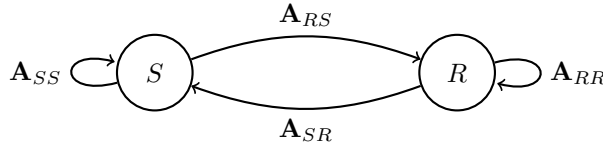


Fig. 1: Partitioned master equation transitions between the truncated set S and the remainder R . Here, \mathbf{A}_{SS} and \mathbf{A}_{RR} represent transitions within S and R , respectively, while \mathbf{A}_{SR} and \mathbf{A}_{RS} represent transitions between them.

3.3.1. Pruning Error in the ℓ^1 -Norm. When pruning a subset $\mathcal{R} \subset S$ of probability mass m , the post-pruning vector is renormalized to maintain a total probability of 1. The following proposition summarizes the effect of this removal on the ℓ^1 -norm.

PROPOSITION 3.4 (Pruning-Induced Error Bound). *Let $\mathcal{R} \subset S$ be the set of pruned states, with total probability mass*

$$m = \sum_{x \in \mathcal{R}} p(x, t).$$

If $\tilde{\mathbf{p}}(t)$ is the renormalized probability vector after removing \mathcal{R} , then

$$\|\mathbf{p}(t) - \tilde{\mathbf{p}}(t)\|_1 \leq 2m.$$

Proof. Let \mathcal{R} be the set of states to be pruned, with total probability

$$m = \sum_{x \in \mathcal{R}} p(x, t).$$

Define the intermediate vector

$$p'(x, t) = \begin{cases} p(x, t), & x \notin \mathcal{R}, \\ 0, & x \in \mathcal{R}, \end{cases}$$

and let

$$\tilde{\mathbf{p}}(t) = \frac{\mathbf{p}'(t)}{1 - m}$$

be the renormalized distribution.

By definition, $\|\mathbf{p}(t) - \mathbf{p}'(t)\|_1 = m$. For the difference between $\mathbf{p}'(t)$ and $\tilde{\mathbf{p}}(t)$, we have:

$$\|\mathbf{p}'(t) - \tilde{\mathbf{p}}(t)\|_1 = \left\| \mathbf{p}'(t) - \frac{\mathbf{p}'(t)}{1 - m} \right\|_1 = \|\mathbf{p}'(t)\|_1 \left| 1 - \frac{1}{1 - m} \right| = (1 - m) \frac{m}{1 - m} = m. \quad \blacksquare$$

By the triangle inequality,

$$\|\mathbf{p}(t) - \tilde{\mathbf{p}}(t)\|_1 \leq \|\mathbf{p}(t) - \mathbf{p}'(t)\|_1 + \|\mathbf{p}'(t) - \tilde{\mathbf{p}}(t)\|_1 = m + m = 2m. \quad \square$$

Remark 3.5. In quantile-based pruning with fraction α , the total pruned probability mass m is typically close to α . Due to potential ties near the threshold, we may have $m \approx \alpha$ or slightly above. This relationship between m and α is crucial when tight control over the truncated mass is required. The error bound of $2m \approx 2\alpha$ directly relates the pruning fraction to the resulting error.

3.3.2. Time Evolution of the Pruning Error. In discrete time stepping, one must also bound how the ℓ^1 -error from pruning propagates forward. The following proposition provides an important property of CME generators.

PROPOSITION 3.6 (Nonexpansiveness of the CME Generator). *Let \mathbf{A} be the generator matrix of a Chemical Master Equation (CME) defined on a state space S , so that $A_{ij} \geq 0$ for $i \neq j$ and $\sum_i A_{ij} = 0$ for every j . Then, for any vector $\mathbf{v} \in \mathbb{R}^{|S|}$ and for all $t \geq 0$,*

$$\|\exp(\mathbf{A} t) \mathbf{v}\|_1 = \|\mathbf{v}\|_1.$$

Proof. For sufficiently small $\delta t > 0$, define $\mathbf{M} = \mathbf{I} + \delta t \mathbf{A}$. Since $A_{ij} \geq 0$ for $i \neq j$ and $\sum_i A_{ij} = 0$, we have $(\mathbf{M})_{ij} = \delta_{ij} + \delta t A_{ij} \geq 0$ and

$$\sum_i (\mathbf{M})_{ij} = 1 + \delta t \sum_i A_{ij} = 1.$$

Thus, \mathbf{M} is column-stochastic, and it follows that $\|\mathbf{M} \mathbf{v}\|_1 = \|\mathbf{v}\|_1$ for any $\mathbf{v} \in \mathbb{R}^{|S|}$. Since the matrix exponential is defined by

$$\exp(\mathbf{A} t) = \lim_{n \rightarrow \infty} \left(\mathbf{I} + \frac{t}{n} \mathbf{A} \right)^n,$$

each factor in the product preserves the ℓ^1 -norm, so by continuity,

$$\|\exp(\mathbf{A} t) \mathbf{v}\|_1 = \|\mathbf{v}\|_1. \quad \square$$

We now use this nonexpansiveness property to show that if a pruning event introduces an error at time t , this error is not amplified during subsequent time steps.

THEOREM 3.7 (Error Propagation in Time Evolution). *Let $\mathbf{p}(t)$ be the exact solution of the CME and let $\tilde{\mathbf{p}}(t)$ be an approximation satisfying*

$$\|\mathbf{p}(t) - \tilde{\mathbf{p}}(t)\|_1 \leq 2m,$$

where $2m$ is the local error from pruning (as established in Proposition 3.4). Then, for any $\Delta t > 0$,

$$\|\mathbf{p}(t + \Delta t) - \exp(\mathbf{A} \Delta t) \tilde{\mathbf{p}}(t)\|_1 \leq 2m.$$

In other words, the error introduced by pruning is not amplified by the time evolution.

Proof. Since $\mathbf{p}(t + \Delta t) = \exp(\mathbf{A} \Delta t) \mathbf{p}(t)$, we have:

$$\begin{aligned} \|\mathbf{p}(t + \Delta t) - \exp(\mathbf{A} \Delta t) \tilde{\mathbf{p}}(t)\|_1 &= \|\exp(\mathbf{A} \Delta t) \mathbf{p}(t) - \exp(\mathbf{A} \Delta t) \tilde{\mathbf{p}}(t)\|_1 \\ &= \|\exp(\mathbf{A} \Delta t)(\mathbf{p}(t) - \tilde{\mathbf{p}}(t))\|_1. \end{aligned}$$

By Proposition 3.6, the matrix exponential preserves the ℓ^1 -norm, so:

$$\|\exp(\mathbf{A} \Delta t)(\mathbf{p}(t) - \tilde{\mathbf{p}}(t))\|_1 = \|\mathbf{p}(t) - \tilde{\mathbf{p}}(t)\|_1 \leq 2m. \quad \square$$

3.3.3. Matrix Exponential Approximation Error. In addition to state-space truncation (and the associated pruning and renormalization error), we approximate the matrix exponential $\exp(\mathbf{A}_S \delta t)$ or, equivalently, employ an ODE solver to advance the solution.

PROPOSITION 3.8 (Local Time-Stepping Error). *For a matrix exponential approximation with tolerance ϵ_{time} , the error in a single time step is bounded by*

$$\left\| \exp(\mathbf{A}_S \delta t) \mathbf{v} - \text{Approx}(\mathbf{A}_S, \delta t) \mathbf{v} \right\|_1 \leq \epsilon_{\text{time}} \|\mathbf{v}\|_1.$$

Modern Krylov subspace implementations like EXPOKIT [16] provide built-in mechanisms to adaptively control this error by adjusting the Krylov subspace dimension based on the specified tolerance.

3.4. Combined Error Control. We now combine the error from state-space truncation (including the pruning and renormalization step) with the error from time-stepping. Our local analysis (see Proposition 3.4 and Theorem 3.7) shows that if at time t the exact probability vector $\mathbf{p}(t)$ is replaced by a pruned and renormalized vector $\tilde{\mathbf{p}}(t)$, then

$$\|\mathbf{p}(t) - \tilde{\mathbf{p}}(t)\|_1 \leq 2m,$$

where m is the total probability mass removed, and this local error is not amplified during the subsequent time step.

Remark 3.9 (Error Allocation Strategy). To achieve optimal efficiency in the FSP algorithm with quantile-based pruning, the time-stepping error should be balanced with the pruning error. Given a pruning fraction α that introduces a truncation error of at most 2α (since typically $m \approx \alpha$), the time-stepping tolerance ϵ_{time} should be set such that

$$\epsilon_{\text{time}} \leq 2\alpha.$$

This ensures that neither error source dominates the computation, allowing both the state space size and Krylov subspace dimension to be minimized while maintaining accuracy.

THEOREM 3.10 (Global Error Bound for FSP with Quantile-Based Pruning). *Let $\mathbf{p}(t) = \exp(\mathbf{A}t)\mathbf{p}(0)$ denote the exact solution of the CME on the full state space, and $\tilde{\mathbf{p}}(t)$ represent the solution computed by the FSP algorithm employing quantile-based pruning. Then the global error accumulated after $N = T/\delta t$ time steps satisfies*

$$\|\mathbf{p}(T) - \tilde{\mathbf{p}}(T)\|_1 \leq N \cdot (2\alpha + \epsilon_{\text{time}}).$$

For a desired global error tolerance ϵ_{global} , the following condition must hold:

$$\frac{T}{\delta t}(2\alpha + \epsilon_{\text{time}}) \leq \epsilon_{\text{global}}.$$

If $\epsilon_{\text{time}} \leq 2\alpha$, this simplifies to

$$\frac{T}{\delta t} \cdot 4\alpha \leq \epsilon_{\text{global}}.$$

Proof. At each discrete time step $t_k = k\delta t$ for $k = 1, \dots, N$, the solution is updated via $\tilde{\mathbf{p}}(t_k) = \text{Approx}(\mathbf{A}_{S_k}, \delta t) \tilde{\mathbf{p}}(t_{k-1})$, where $\text{Approx}(\mathbf{A}_{S_k}, \delta t)$ approximates $\exp(\mathbf{A}_{S_k} \delta t)$ within tolerance ϵ_{time} , and S_k is the truncated state space resulting from pruning. Two primary sources contribute to the local error. First, quantile-based pruning and renormalization remove at most $m_k \approx \alpha$ probability mass, yielding a local truncation error of at most 2α . Second, the approximation of the matrix exponential introduces an additional error bounded by ϵ_{time} . Summing these errors over N time steps leads directly to the stated global error bound. \square

3.5. State Space Update. In an adaptive simulation the truncated state space is updated at each iteration: some states are removed (pruned) and new states are discovered and added. Let $\mathbf{X}_S^{\text{old}}$ denote the current truncated state space. Suppose that at a given update step a set $\mathcal{R} \subset \mathbf{X}_S^{\text{old}}$ is pruned and a set \mathcal{S}_{new} of new states is added. Then the updated state space is given by

$$\mathbf{X}_S^{\text{updated}} = (\mathbf{X}_S^{\text{old}} \setminus \mathcal{R}) \cup \mathcal{S}_{\text{new}}.$$

Correspondingly, the CME generator matrix must be updated to reflect the new set of states and the associated transitions.

3.5.1. Transition Matrix Reconstruction Algorithm. Algorithm 3.2 provides a blockwise procedure to update the generator matrix when the state space is modified by both pruning and expansion. Instead of recomputing the entire matrix from scratch, we partition the current state space into the retained set S and the pruned set R (see Remark 3.3 and Figure 1). First, we extract the submatrix corresponding to S from the current generator matrix A_{old} . Then, we append new rows and columns for the newly discovered states, computing the transition rates between the retained states and the new states using the reaction rules and propensity functions. This block-wise update guarantees that the new generator matrix $\mathbf{A}_{\text{updated}}$ retains the correct structure.

After the state-space update, the new generator matrix $\mathbf{A}_{\text{updated}}$ satisfies the usual properties of a CME generator:

$$A_{jj} = - \sum_{\substack{i \in \mathbf{X}_S^{\text{updated}} \\ i \neq j}} A_{ij}, \quad A_{ij} \geq 0 \text{ for } i \neq j,$$

ensuring that each column sums to zero and all off-diagonal entries are nonnegative, thus conserving probability.

Algorithm 3.2 Transition Matrix Reconstruction for Adaptive State Space

Require: $\mathbf{A}_{\text{current}}$: Current transition matrix for state space $\mathbf{X}_S^{\text{old}}$
 \mathcal{R} : Set of states to be removed (pruned)
 \mathcal{S}_{new} : Set of new states to be added
 Reactions: List of reactions with their propensity functions

- 1: Define the retained state space: $\mathbf{X}_S^{\text{ret}} = \mathbf{X}_S^{\text{old}} \setminus \mathcal{R}$
- 2: Form the intermediate matrix \mathbf{A}_{ret} by extracting the rows and columns of $\mathbf{A}_{\text{current}}$ corresponding to $\mathbf{X}_S^{\text{ret}}$
- 3: Initialize $\mathbf{A}_{\text{updated}}$ as a sparse zero matrix of size $(|\mathbf{X}_S^{\text{ret}}| + |\mathcal{S}_{\text{new}}|) \times (|\mathbf{X}_S^{\text{ret}}| + |\mathcal{S}_{\text{new}}|)$
- 4: Copy \mathbf{A}_{ret} into the top-left block of $\mathbf{A}_{\text{updated}}$
- 5: **for** each new state $s_k \in \mathcal{S}_{\text{new}}$ **do**
- 6: **for** each reaction $r \in \text{Reactions}$ **do**
- 7: Determine the change vector $\boldsymbol{\nu}_r$ associated with reaction r
- 8: Identify all states $s_j \in \mathbf{X}_S^{\text{ret}}$ such that a transition $s_j \rightarrow s_k$ is possible via r
- 9: **if** such a state s_j exists **then**
- 10: Set $\mathbf{A}_{\text{updated}}[k, j] \leftarrow a_r(s_j)$ (transition from s_j to s_k)
- 11: **end if**
- 12: Similarly, update entries for transitions from the new state s_k to retained states.
- 13: **end for**
- 14: **end for**
- 15: Adjust the diagonal entries of $\mathbf{A}_{\text{updated}}$ so that for every state $s_j \in \mathbf{X}_S^{\text{updated}}$,

$$A_{jj} = - \sum_{\substack{i \in \mathbf{X}_S^{\text{updated}} \\ i \neq j}} A_{ij}.$$

16: **return** $\mathbf{A}_{\text{updated}}$

3.6. FSP Algorithm with Quantile-Based Pruning. In summary, the adaptive state-space update consists of three complementary operations:

- **Expansion:** Newly discovered states are added and the transition matrix is updated accordingly (using Algorithm 3.2), while ensuring that each column of the updated matrix sums to zero.
- **Time Evolution:** The probability distribution is evolved in the expanded space by solving the matrix exponential.
- **Pruning:** A controlled fraction α of the probability mass is removed (using quantile-based pruning), with theoretical bounds (e.g., Proposition 3.4) ensuring that the ℓ^1 -error remains bounded.

These operations, together with the error bound analysis (Proposition 3.4 and Theorem 3.10), guarantee that the overall simulation remains consistent with the probabilistic framework and that the global error is controlled.

To put our theoretical framework into practice, we present the *FSP Algorithm with Quantile-Based Pruning* (Algorithm 3.3). This algorithm utilizes the global error bound (Theorem 3.10) and applies quantile-based pruning to dynamically manage the state space while ensuring error control.

Algorithm 3.3 Finite State Projection (FSP) with Quantile-Based Pruning

-
- 1: **Inputs:** Time interval (t_0, t_f) , initial state \mathbf{x}_0 with $\mathbf{p}(\{\mathbf{x}_0\}, t_0) = 1$, global error tolerance ϵ_{global} , fixed time step δt , pruning fraction α , and time-stepping tolerance $\epsilon_{\text{time}} \leq 2\alpha$, Expansion factor r .
 - 2: Initialize time: $t \leftarrow t_0$.
 - 3: Initialize truncated state space: $\mathbf{X}_S \leftarrow \{\mathbf{x}_0\}$.
 - 4: Initialize probability vector: $\mathbf{p}(\mathbf{X}_S, t_0) \leftarrow [1]$.
 - 5: **Verify error tolerance:** Confirm that $\frac{t_f - t_0}{\delta t} \cdot (2\alpha + \epsilon_{\text{time}}) \leq \epsilon_{\text{global}}$.
 - 6: **while** $t < t_f$ **do**
 - 7: **Expand state space:** Add new states reachable from the current boundary:

$$\mathcal{S}_{\text{new}} = \{\text{states reachable from current boundary in } r \text{ steps}\}$$

$$\mathbf{X}_S \leftarrow \mathbf{X}_S \cup \mathcal{S}_{\text{new}}$$
 - 8: Update the generator matrix \mathbf{A}_S to include the new states (see Algorithm 3.2).
 - 9: **Evolve in time:** Propagate the probability distribution from t to $t + \delta t$ using a matrix exponential approximation with tolerance ϵ_{time} :

$$\mathbf{p}(\mathbf{X}_S, t + \delta t) \approx \exp(\mathbf{A}_S \delta t) \mathbf{p}(\mathbf{X}_S, t).$$
 - 10: **Prune via Quantile Threshold α :** Apply Algorithm 3.1 to remove the bottom α -fraction of states by probability mass and renormalize the remaining probabilities.
 - 11: **Update time:** $t \leftarrow t + \delta t$.
 - 12: **end while**
 - 13: **Output:** The final probability vector $\mathbf{p}(\mathbf{X}_S, t_f)$ and the final truncated state set \mathbf{X}_S .
-

4. Experimental Setup. Our implementation uses the quantile-based pruning strategy with error allocation to ensure both accuracy and computational efficiency. The practical implementation follows the error allocation principles established in Remark 3.9.

Remark 4.1 (Error Allocation Strategy). To achieve a balanced performance in the FSP algorithm with quantile-based pruning, it makes sense to balance the time-stepping error with the pruning error. In particular, if a pruning fraction α introduces a local truncation error of at most 2α , a reasonable approach is to set the time-stepping tolerance ϵ_{time} such that

$$\epsilon_{\text{time}} \leq 2\alpha.$$

All simulations were implemented in **Julia** [1], using **Catalyst.jl** [4] for reaction network modeling and **ExpoKit.jl** [7] for computing matrix exponentials via Krylov subspace methods. The matrix exponential calculations leverage **ExpoKit.jl**'s built-in error control mechanisms, with the time-stepping tolerance set according to the error allocation strategy above. The FSP algorithm with quantile-based pruning dynamically adjusted the truncated state space by performing state expansions when probability mass approached the boundary and applying quantile-based pruning to remove low-probability states while ensuring error control. Each model was simulated with appropriate expansion strategies and fixed time steps to balance computational efficiency and accuracy. The global error tolerance was verified to satisfy:

$$\frac{T}{\delta t} \cdot 4\alpha \leq \epsilon_{\text{global}}$$

4.1. Comparison with SSA. To validate the accuracy of our FSP approach with quantile-based pruning, we compared its results against the stochastic simulation algorithm (SSA), which serves as a benchmark for the true system dynamics. For both the Lotka–Volterra and Michaelis–Menten models, 1000 independent SSA trajectories were generated. The ensemble mean was obtained by linearly interpolating the individual SSA trajectories at common time points and then averaging them, thereby providing a robust reference for the system dynamics.

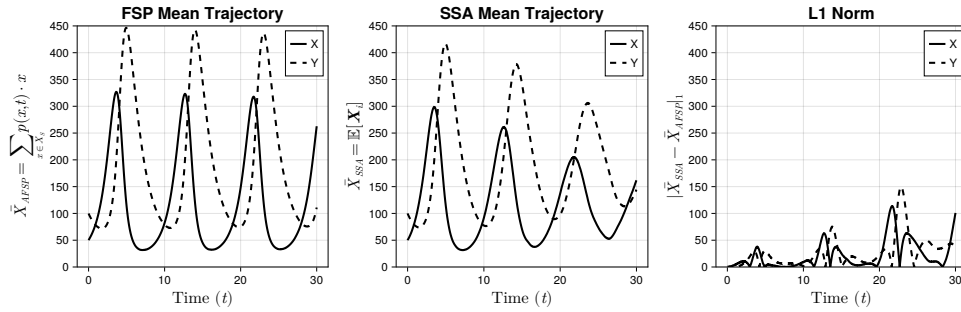


Fig. 2: Comparison of mean trajectories for the Lotka–Volterra model: FSP with quantile-based pruning vs. SSA (1000 realizations). The two methods produce nearly identical results.

Similar comparisons for the Michaelis–Menten enzyme kinetics model (see Figures in Section 5) indicate that the FSP with quantile-based pruning reliably reproduces the SSA ensemble averages. Detailed implementations and experiments are available at <https://github.com/AdityaDendukuri/DiscStochSim.jl>.

5. Results. We evaluate the performance of the FSP approach with quantile-based pruning on three benchmark models: the *Lotka–Volterra (Predator–Prey) Model*, *Michaelis–Menten Enzyme Kinetics*, and the *Stochastic Toggle Switch Model*. Each system presents unique challenges, including oscillatory behavior, nonlinear reaction kinetics, and bimodal probability distributions, making them excellent tests for adaptive state-space truncation. Figure 3 illustrates how the algorithm maintains bounded truncation error while adapting the state space size in response to probability distribution changes. The results confirm that the error remains well-controlled, supporting the theoretical bounds developed in Proposition 3.4.

5.1. Lotka–Volterra (Predator–Prey) Model. The Lotka–Volterra model describes a simple predator-prey interaction where prey (X_1) reproduce, predators (X_2) consume prey, and predators eventually die. This results in cyclic population dynamics: as prey abundance increases, the predator population also grows due to increased food availability. However, as predators overconsume prey, the prey population declines, leading to a subsequent drop in predators. This oscillatory cycle repeats with stochastic variations. Table 1 summarizes the reaction network for this system.

In our simulation, the initial population was set to $(X_1, X_2) = (50, 100)$, with rate parameters $(a, b, c) = (0.1, 0.005, 0.6)$. The state space expanded approximately

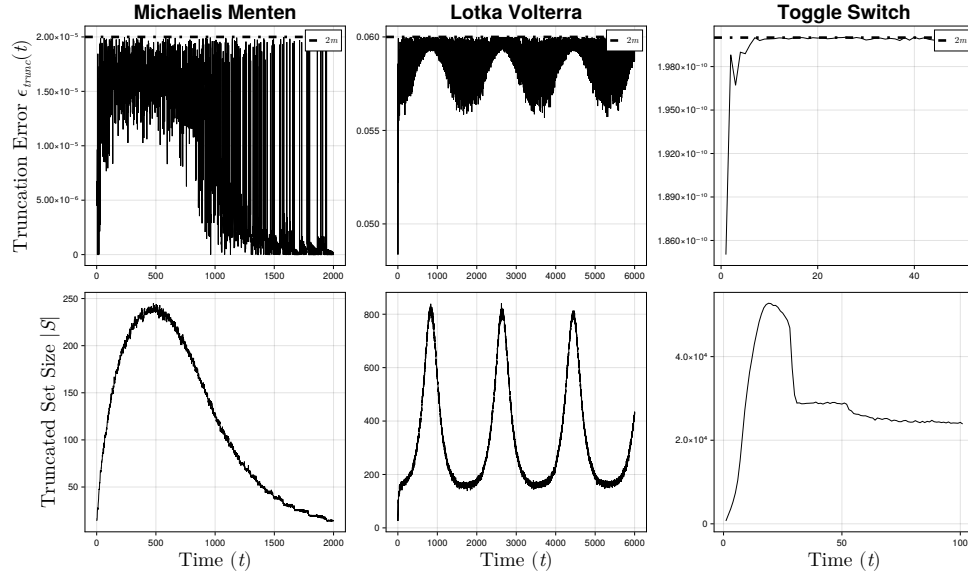


Fig. 3: Local truncation error (top row) and the size of the truncated state space (bottom row) for the three benchmark models. The results confirm that (i) the local error remains bounded by $2m$, where m is the total mass pruned at each step, and (ii) the state space dynamically adapts to the evolving probability distribution, efficiently capturing relevant states while discarding negligible ones.

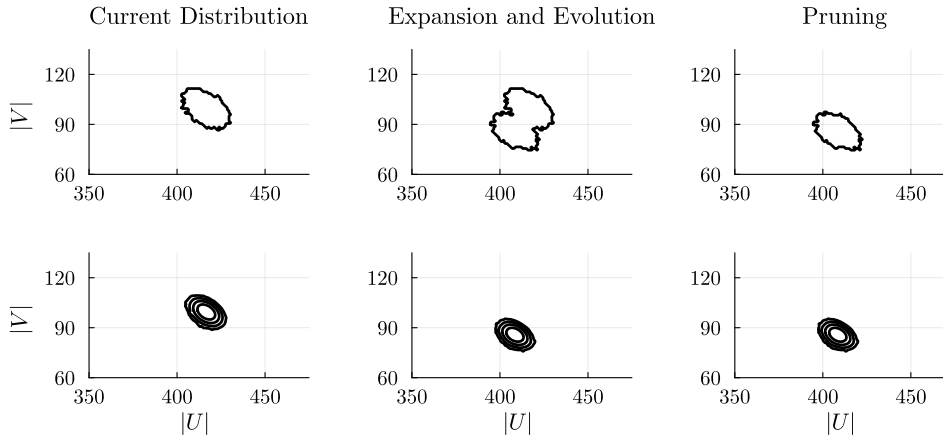


Fig. 4: A single iteration of the adaptive FSP procedure for the Lotka–Volterra model. The top row displays the active states at each stage (before expansion, after time evolution, and after pruning), while the bottom row shows the corresponding probability distribution $p(x, t)$.

three reaction steps per time step, efficiently adapting to probability mass movement. The full simulation completed in **90 seconds**. Figure 4 illustrates the three main

Reaction	Reaction Equation	Propensity	Stoichiometric Vector
1	$X_1 \xrightarrow{a} 2X_1$	$a \cdot X_1$	$\begin{bmatrix} 1 \\ 0 \end{bmatrix}$
2	$X_1 + X_2 \xrightarrow{b} 2X_2$	$b \cdot X_1 \cdot X_2$	$\begin{bmatrix} -1 \\ 1 \end{bmatrix}$
3	$X_2 \xrightarrow{c} \emptyset$	$c \cdot X_2$	$\begin{bmatrix} 0 \\ -1 \end{bmatrix}$

Table 1: Reactions, propensities, and stoichiometric vectors for the Lotka–Volterra model.

operations (expansion, time evolution, and pruning) for the Lotka–Volterra model in a single iteration of our adaptive FSP procedure. The left panel shows the current probability distribution, the middle panel captures the expanded state space and its short-term evolution, and the right panel depicts the result of pruning low-probability states.

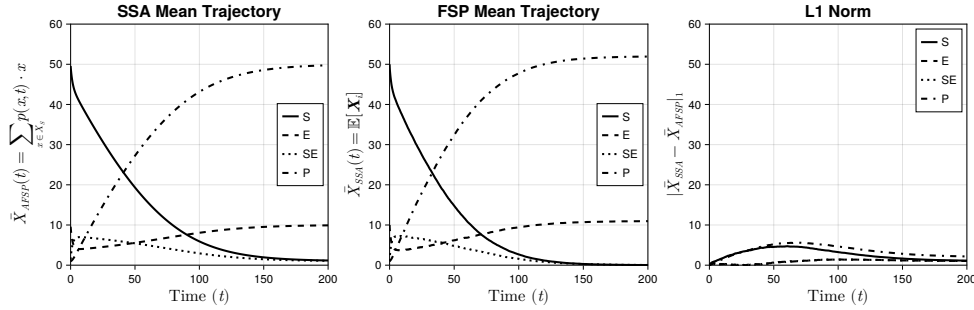


Fig. 5: Comparison of mean trajectories for the Michaelis–Menten system: FSP with quantile-based pruning vs. SSA (1000 realizations). The FSP solution closely matches the SSA ensemble average, confirming its accuracy.

5.2. Michaelis–Menten Enzyme Kinetics. The Michaelis–Menten (MM) model describes enzyme-catalyzed reactions where a substrate (S) binds with an enzyme (E) to form an intermediate complex (ES), which then produces a product (P). The system exhibits transient dynamics before reaching a quasi-equilibrium state, where the enzyme-substrate complex maintains a steady concentration as the reaction proceeds. This reaction network, given in Table 2, captures both the transient dynamics and the quasi-equilibrium behavior of enzyme kinetics.

Our simulation started with initial values $(E, S, ES, P) = (50, 10, 1, 1)$ and rate parameters $(k_1, k_{-1}, k_2) = (0.01, 0.1, 0.1)$. The state space expanded by approximately two reaction steps per time step. The simulation ran efficiently, completing in **8 seconds**. Figure 5 compares the mean trajectory computed using FSP with quantile-based pruning with an SSA simulation over 1000 realizations. The close agreement confirms that our method accurately captures the transient and steady-state behavior of the enzyme reaction while dynamically adjusting state-space size.

Reaction	Reaction Equation	Propensity	Stoichiometric Vector
1	$E + S \xrightarrow{k_1} ES$	$k_1 \cdot E \cdot S$	$\begin{bmatrix} -1 \\ -1 \\ +1 \\ 0 \end{bmatrix}$
2	$ES \xrightarrow{k_{-1}} E + S$	$k_{-1} \cdot ES$	$\begin{bmatrix} +1 \\ +1 \\ -1 \\ 0 \end{bmatrix}$
3	$ES \xrightarrow{k_2} E + P$	$k_2 \cdot ES$	$\begin{bmatrix} +1 \\ 0 \\ -1 \\ +1 \end{bmatrix}$

Table 2: Reactions, propensities, and stoichiometric vectors for the Michaelis–Menten enzyme kinetics model. The state vector is (E, S, ES, P) .

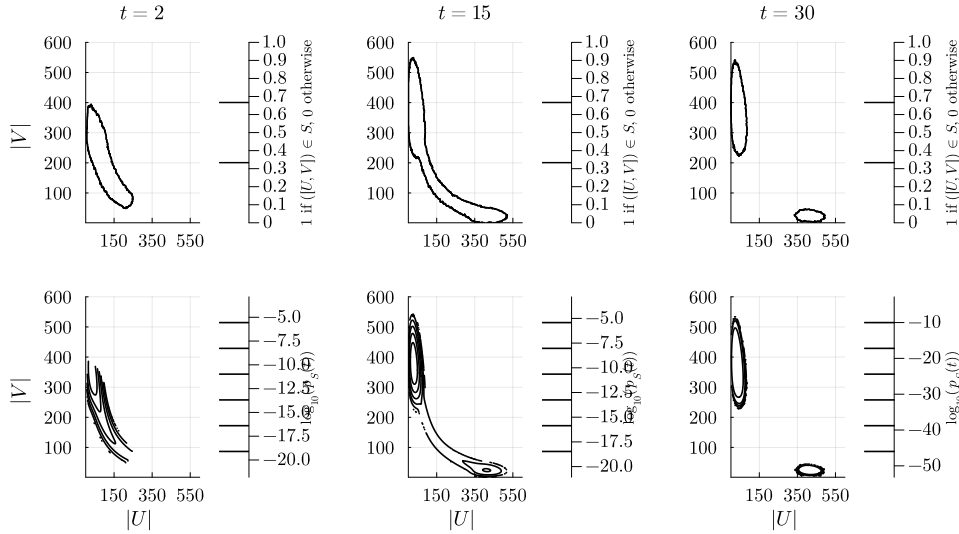


Fig. 6: Joint probability distribution of the stochastic toggle switch at $t \approx 28$. The algorithm successfully identifies the two stable regions corresponding to the bimodal steady-state distribution.

5.3. Stochastic Toggle Switch Model. The stochastic toggle switch is a genetic regulatory network where two mutually repressive proteins (U and V) compete for dominance [18]. The system exhibits bistability, meaning that probability mass accumulates in two separate regions corresponding to high expression of one protein and low expression of the other. Noise-driven transitions between these states occur over time, making adaptive state-space expansion crucial for capturing rare switching events. Table 3 details the reaction network.

In our simulation, the initial values were $(U, V) = (85, 5)$, and the reaction rate

Reaction	Reaction Equation	Propensity	Stoichiometric Vector
1	$\emptyset \xrightarrow{\eta\left(\alpha_1 + \frac{\beta_1 K_1^3}{K_1^3 + V^3}\right)} U$	$\eta\left(\alpha_1 + \frac{\beta_1 K_1^3}{K_1^3 + V^3}\right)$	+1
2	$U \xrightarrow{d_1 + \frac{s\gamma}{1+s}} \emptyset$	$d_1 + \frac{s\gamma}{1+s}$	-1
3	$\emptyset \xrightarrow{\eta\left(\alpha_2 + \frac{\beta_2 K_2^3}{K_2^3 + U^3}\right)} V$	$\eta\left(\alpha_2 + \frac{\beta_2 K_2^3}{K_2^3 + U^3}\right)$	+1
4	$V \xrightarrow{d_2} \emptyset$	d_2	-1

Table 3: Reactions, propensities, and stoichiometric vectors for the stochastic toggle switch model [18, 13]. Here, the forward reactions incorporate Hill-type kinetics to capture mutual repression, and the reverse reactions represent degradation.

parameters were taken from [13]. Figure 6 shows the probability distribution at $t \approx 28$, where two well-separated peaks illustrate the bimodal steady-state behavior. The FSP algorithm with quantile-based pruning successfully tracks both stable regions, dynamically expanding the state space when probability mass moves between them and pruning irrelevant states. This result highlights the method’s effectiveness in capturing complex stochastic dynamics without excessive computational overhead.

The results confirm that our method accurately captures the main stochastic dynamics while significantly reducing computational cost. Unlike SSA, which requires thousands of trajectories to compute a reliable mean, the FSP with quantile-based pruning directly produces a full probability distribution and adapts the state space dynamically. This not only yields an accurate mean trajectory but also provides additional insight into the probability distribution of the system.

6. Conclusions. In this paper, we introduced an adaptive Finite State Projection (FSP) method for solving the Chemical Master Equation (CME) in stochastic reaction networks. By incorporating quantile-based pruning and controlled state expansion, we aimed to retain only the most relevant states while maintaining rigorous error bounds. Our approach ensures that the error at each step remains proportional to the pruned probability mass, which is controlled by the user, preventing unchecked accumulation over time. We evaluated the method on benchmark models, including the Lotka–Volterra system, Michaelis–Menten enzyme kinetics, and a stochastic toggle switch. The results indicate that adaptive FSP captures key stochastic dynamics while significantly reducing computational cost compared to standard FSP approaches. The use of Krylov subspace methods for matrix exponential approximations further improved efficiency in time integration. Overall, our approach provides a flexible framework for modeling stochastic biochemical systems with evolving state spaces. While it does not eliminate all challenges associated with state truncation, it offers a practical balance between accuracy and computational feasibility, making it a useful tool for analyzing complex stochastic systems in systems biology and related fields.

REFERENCES

- [1] J. BEZANSON, A. EDELMAN, S. KARPINSKI, AND V. B. SHAH, *Julia: A fresh approach to numerical computing*, SIAM Review, 59 (2017), pp. 65–98.

- [2] K. BURRAGE, M. HEGLAND, S. MACNAMARA, AND R. B. SIDJE, *A krylov-based finite state projection algorithm for solving the chemical master equation arising in the discrete modelling of biological systems*, 2006, <https://api.semanticscholar.org/CorpusID:115616271>.
- [3] Y. CAO, J. LIANG, D. PETTIGREW, AND S. KOU, *Adaptive aggregation of state-space models for the chemical master equation*, Multiscale Modeling & Simulation, 14 (2016), pp. 28–48.
- [4] CATALYST.JL DEVELOPMENT TEAM, *Catalyst.jl – modeling chemical reaction networks*. <https://catalyst.sciml.ai>, 2021. Accessed: 2025-03-16.
- [5] K. N. DINH AND R. B. SIDJE, *Understanding the finite state projection and related methods for solving the chemical master equation*, Physical Biology, 13 (2016), p. 035003.
- [6] T. DINH AND R. B. SIDJE, *An adaptive solution to the chemical master equation using quantized tensor trains with sliding windows*, Physical Biology, 17 (2020), p. 065014, <https://doi.org/10.1088/1478-3975/aba1d2>, <https://dx.doi.org/10.1088/1478-3975/aba1d2>.
- [7] EXPOKIT.JL DEVELOPMENT TEAM, *Expokit.jl – efficient matrix exponential computations in julia*. <https://github.com/SciML/Expokit.jl>, 2021. Accessed: 2025-03-16.
- [8] D. T. GILLESPIE, *Exact stochastic simulation of coupled chemical reactions*, The Journal of Physical Chemistry, 81 (1977), pp. 2340–2361.
- [9] D. T. GILLESPIE, *Approximate accelerated stochastic simulation of chemically reacting systems*, The Journal of Chemical Physics, 115 (2001), pp. 1716–1733.
- [10] T. JAHNKE, *Adaptive wavelet methods for the efficient solution of the chemical master equation*, SIAM Journal on Scientific Computing, 31 (2010), pp. 4373–4394.
- [11] V. KAZEED, M. KHAMMASH, AND M. NIP, *Direct solution of the chemical master equation using tensor trains*, PLoS Computational Biology, 10 (2014), p. e1003359.
- [12] J. KIM, J. DARK, G. ENCISO, AND S. SINDI, *Slack reactants: A state-space truncation framework to estimate quantitative behavior of the chemical master equation*, J. Chem. Phys., 153 (2020), p. 054117.
- [13] S. MACNAMARA, K. BURRAGE, AND R. B. SIDJE, *Multiscale modeling of chemical kinetics via the master equation*, Multiscale Modeling & Simulation, 6 (2008), pp. 1146–1168, <https://doi.org/10.1137/060678154>, <https://doi.org/10.1137/060678154>, <https://arxiv.org/abs/https://doi.org/10.1137/060678154>.
- [14] B. MUNSKY AND M. KHAMMASH, *Finite state projection for the solution of the chemical master equation*, The Journal of Chemical Physics, 124 (2006), p. 044104.
- [15] B. MUNSKY AND M. KHAMMASH, *A multiple time interval finite state projection algorithm for the solution to the chemical master equation*, Journal of Computational Physics, 226 (2007), pp. 818–835, <https://doi.org/https://doi.org/10.1016/j.jcp.2007.05.016>, <https://www.sciencedirect.com/science/article/pii/S0021999107002100>.
- [16] R. B. SIDJE, *Expokit: A software package for computing matrix exponentials*, ACM Transactions on Mathematical Software, 24 (1998), pp. 130–156.
- [17] V. SUNKARA AND M. HEGLAND, *An optimal finite state projection method*, Procedia CS, 1 (2010), pp. 1579–1586, <https://doi.org/10.1016/j.procs.2010.04.177>.
- [18] T. TIAN AND K. BURRAGE, *Stochastic models for regulatory networks of the genetic toggle switch*, Proceedings of the National Academy of Sciences, 103 (2006), pp. 8372–8377, <https://doi.org/10.1073/pnas.0507818103>, <https://www.pnas.org/doi/abs/10.1073/pnas.0507818103>. eprint: <https://www.pnas.org/doi/pdf/10.1073/pnas.0507818103>.
- [19] H. VO AND R. SIDJE, *Improved krylov-fsp method for solving the chemical master equation*, 10 2016.
- [20] H. D. VO AND R. B. SIDJE, *An adaptive solution to the chemical master equation using tensors*, The Journal of Chemical Physics, 147 (2017), p. 044102, <https://doi.org/10.1063/1.4994917>, <https://doi.org/10.1063/1.4994917>, <https://arxiv.org/abs/https://pubs.aip.org/aip/jcp/article-pdf/doi/10.1063/1.4994917/15530015/044102.1.online.pdf>.
- [21] V. WOLF, R. GOEL, M. MATEESCU, AND T. A. HENZINGER, *Solving the chemical master equation using sliding windows*, BMC Syst. Biol., 4 (2010), p. 42.